

# Cyclic Prefixing or Zero Padding for Wireless Multicarrier Transmissions?

Bertrand Muquet, *Member, IEEE*, Zhengdao Wang, *Student Member, IEEE*, Georgios B. Giannakis, *Fellow, IEEE*, Marc de Courville, *Member, IEEE*, and Pierre Duhamel, *Fellow, IEEE*

**Abstract**—Zero padding (ZP) of multicarrier transmissions has recently been proposed as an appealing alternative to the traditional cyclic prefix (CP) orthogonal frequency-division multiplexing (OFDM) to ensure symbol recovery regardless of the channel zero locations. In this paper, both systems are studied to delineate their relative merits in wireless systems where channel knowledge is not available at the transmitter. Two novel equalizers are developed for ZP-OFDM to tradeoff performance with implementation complexity. Both CP-OFDM and ZP-OFDM are then compared in terms of transmitter nonlinearities and required power backoff. Next, both systems are tested in terms of channel estimation and tracking capabilities. Simulations tailored to the realistic context of the standard for wireless local area network HIPERLAN/2 illustrate the pertinent tradeoffs.

**Index Terms**—Channel estimation, cyclic prefix, equalization, HIPERLAN/2, IEEE 802.11a, orthogonal frequency-division multiplexing (OFDM), zero padding.

## I. INTRODUCTION

**T**HOUGH unnoticed for some time, there has been an increasing interest toward multicarrier and, in particular, orthogonal frequency-division multiplexing (OFDM), not only for digital audio broadcasting (DAB) and digital video broadcasting (DVB) [2], [3], but also for high-speed modems over digital subscriber lines (xDSL) [6], and, more recently, for broadband wireless local area networks (ETSI BRAN HIPERLAN/2 harmonized with IEEE 802.11a) [5].

OFDM entails redundant block transmissions and enables very simple equalization of frequency-selective finite impulse response (FIR) channels, thanks to the inverse fast Fourier

transform (IFFT) precoding and the insertion of the so-called cyclic prefix (CP) at the transmitter. At the receiver end, the CP is discarded to avoid interblock interference (IBI) and each truncated block is fast Fourier transform (FFT) processed—an operation converting the frequency-selective channel into parallel flat-faded independent subchannels, each corresponding to a different subcarrier. Unless zero, flat fades are removed by dividing each subchannel's output with the channel transfer function at the corresponding subcarrier. Wireline (e.g., xDSL) systems with channel state information (CSI) at the transmitter bypass channel fades with power loading. But for most wireless applications, CSI is impossible (or too costly) to acquire, leaving error-control coding the task for fading mitigation at the transmitter, a task for which it may not be the right tool [25]. Indeed, at the expense of bandwidth overexpansion, coded OFDM [26] ameliorates performance losses incurred by channels having nulls on (or close to) the transmitted subcarriers, but does not eliminate them.

Hence, it was recently proposed to replace the generally nonzero CP by zero padding (ZP) [11], [18], [24]. Specifically, in each block of the so-termed ZP-OFDM transmission, zero symbols are appended after the IFFT-precoded information symbols. If the number of zero symbols equals the CP length, then ZP-OFDM and CP-OFDM transmissions have the same spectral efficiency. Unlike CP-OFDM and without bandwidth-consuming channel coding, ZP-OFDM guarantees symbol recovery and assures FIR [even zero-forcing (ZF)] equalization of FIR channels *regardless* of the channel zero locations [11], [15], [18]. The price paid is somewhat increased receiver complexity (the single FFT required by CP-OFDM is replaced by FIR filtering).

In this paper, we take a closer look at ZP-OFDM and compare it with CP-OFDM in terms of equalization capabilities, nonlinear amplifier effects, and channel estimation accuracy. We are mainly concerned with wireless applications, where CSI is not available at the transmitter. A brief description of both systems is provided in Section II where notation is also introduced. In Section III, two equalizers are derived that tradeoff bit error rate (BER) performance for extra savings in complexity. The simplest one is motivated by the overlap-add (OLA) method of block convolution and is termed ZP-OFDM-OLA. It has computational complexity equivalent to CP-OFDM, but similar to CP-OFDM, its performance is also sensitive to channel zeros that are close to subcarriers. The second equalizer (ZP-OFDM-FAST) is slightly more complex than CP-OFDM, but similar to ZP-OFDM, it guarantees symbol recovery and offers BER performance close to ZP-OFDM-minimum mean-square error

Paper approved by M. Chiani, the Editor for Wireless Communication of the IEEE Communications Society. Manuscript received September 6, 2000; revised March 15, 2001 and July 15, 2001. This work was supported in part by the National Science Foundation (NSF) under CCR Grant 98-05350 and in part by the NSF under Wireless Initiative Grant 99-79443. This paper was presented in part at the International Conference on Communications, New Orleans, LA, June 2000, and in part at the International Conference on Acoustic, Speech, and Signal Processing, Istanbul, Turkey, June 2000.

B. Muquet was with Motorola Laboratories Paris, Espace Technologique Saint-Aubin, 91193 Gif-sur-Yvette, France. He is now with Stepmind, 92100 Boulogne, France (e-mail: bertrand.muquet@stepmind.com).

M. de Courville is with Motorola Laboratories Paris, Espace Technologique Saint-Aubin, 91193 Gif-sur-Yvette, France (e-mail: courvill@crm.mot.com).

Z. Wang and G. B. Giannakis are with the Department of Electrical and Computer Engineering, University of Minnesota, Minneapolis, MN 55455 USA (e-mail: zhengdao@ece.umn.edu; georgios@ece.umn.edu).

P. Duhamel was with the École Nationale Supérieure des Télécommunications, 75013 Paris, France. He is now with CNRS/LSS, Supélec, 91190 Gif-sur-Yvette, France (e-mail: pierre.duhamel@lss.supelec.fr).

Digital Object Identifier 10.1109/TCOMM.2002.806518

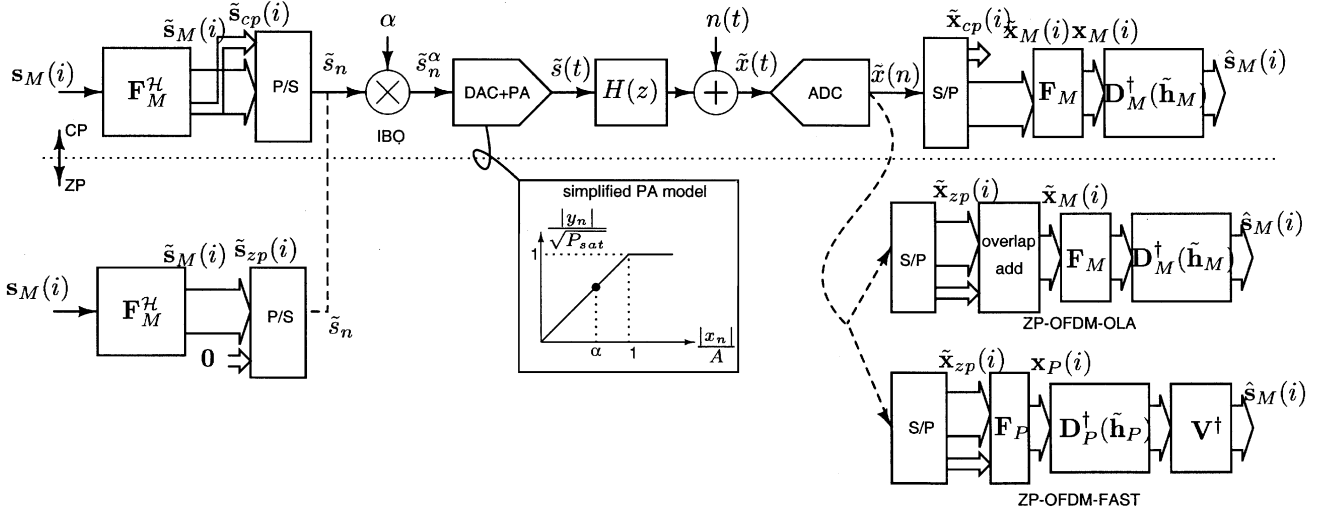


Fig. 1. Discrete-time block equivalent models of CP-OFDM and ZP-OFDM.

(MMSE). The noise color introduced by the various ZP equalizers is also accounted for in Section III to enable a Viterbi decoder with manageable complexity.

In Section IV, the nonlinear distortions introduced by the radio frequency (RF) power amplifier (PA) are taken into account and the peak-to-average power ratio (PAR) is considered as a figure of merit [23] when comparing ZP- with CP-OFDM.

Because linear equalizers require CSI at the receiver, the main aspects of channel estimation is considered in Section V. First, both precoders are compared with respect to CSI acquisition. A novel channel estimator is developed for ZP-OFDM transmissions by extending the pilot-based channel estimator developed in [17] for CP-OFDM. To evaluate channel tracking capabilities, additional comparisons are then performed between two semiblind subspace-based channel estimators developed for the CP and ZP precoders in [16] and [18], and both are also tested against the conventional pilot-based approach. To comply with the HIPERLAN/2 (HL2) standard, some modifications of these algorithms are also developed in order to account for the presence of zero subcarriers, used to provide frequency guard bands between adjacent OFDM systems. In addition to modifying subspace channel estimation algorithms, Section V deals also with their inherent scalar ambiguity by resorting to a semiblind least-squares criterion that incorporates pilot subcarriers.

In Section VI, illustrating simulations are conducted in the realistic context of HL2, while conclusions are drawn in Section VII.

## II. SYSTEMS DESCRIPTION

In this section, we provide a brief overview of the CP-OFDM and ZP-OFDM systems.

### A. Standard CP-OFDM

The upper part of Fig. 1 depicts the baseband discrete-time block equivalent model of a standard CP-OFDM system, where

the  $i$ th  $M \times 1$  information block<sup>1</sup>  $s_M(i)$  is first precoded by the IFFT matrix  $\mathbf{F} = \mathbf{F}_M^{-1} = \mathbf{F}_M^H$  with  $(m, k)$ th entry  $\exp\{j2\pi mk/M\}/\sqrt{M}$ , to yield the so-called “time domain” block vector  $\tilde{s}_M(i) = \mathbf{F}_M^H s_M(i)$ , where  $(\cdot)^H$  denotes conjugate transposition. Then a CP of length  $D$  is inserted between each  $\tilde{s}_M(i)$ . The entries of the resulting redundant block  $\tilde{s}_{cp}(i)$  are finally sent sequentially through the channel. The total number of time-domain samples per transmitted block is, thus,  $P = M + D$ . Consider the  $M \times D$  matrix  $\tilde{\mathbf{F}}_{cp}$  formed by the last  $D$  columns of  $\mathbf{F}_M$ . Defining  $\mathbf{F}_{cp} := [\tilde{\mathbf{F}}_{cp}, \mathbf{F}_M]^H$  as the  $P \times M$  matrix corresponding to the combined multicarrier modulation and CP insertion, the block of symbols to be transmitted can simply be expressed as  $\tilde{s}_{cp}(i) = \mathbf{F}_{cp} s_M(i)$ .

Each block  $\tilde{s}_{cp}(i)$  is then serialized to obtain the time-domain samples  $\tilde{s}_n(i)$ , which are scaled by  $\alpha$  to yield  $\tilde{s}_n^\alpha(i) := \alpha \tilde{s}_n(i)$  and reduce the nonlinear distortions introduced after they pass through the PA. For simplicity, these distortions will be first omitted but their effects will be revisited in Section IV. With  $(\cdot)^T$  denoting transposition, the frequency-selective propagation will be modeled as a FIR filter with channel impulse response (CIR) column vector  $\mathbf{h} := [h_0 \cdots h_{M-1}]^T$  and additive white Gaussian noise (AWGN)  $\tilde{n}_n(i)$  of variance  $\sigma_n^2$ . In practice, the system is designed such that  $M \geq D \geq L$ , where  $L$  is the channel order (i.e.,  $h_i = 0, \forall i > L$ ). No CSI is assumed available at the transmitter. That way, the expression of the  $i$ th received symbol block is given by

$$\tilde{\mathbf{x}}_{cp}(i) = \mathbf{H}\mathbf{F}_{cp}s_M(i) + \mathbf{H}_{IBI}\mathbf{F}_{cp}s_M(i-1) + \tilde{\mathbf{n}}_P(i) \quad (1)$$

where  $\mathbf{H}$  is the  $P \times P$  lower triangular Toeplitz filtering matrix with first column  $[h_0 \cdots h_L \ 0 \cdots 0]^T$ ;  $\mathbf{H}_{IBI}$  is the  $P \times P$  upper triangular Toeplitz filtering matrix with first row  $[0 \cdots 0 \ h_L \cdots h_1]$ , which captures IBI; and  $\tilde{\mathbf{n}}_P(i) := [\tilde{n}(iP) \cdots \tilde{n}(iP + P - 1)]^T$  denotes the AWGN vector.

<sup>1</sup>Boldface symbols are used throughout this paper to denote column vectors (matrices), sometimes with subscripts  $M$  or  $P$  to emphasize their sizes; tildes ( $\tilde{\cdot}$ ) denotes IFFT precoded quantities; and argument  $i$  is used to index blocks of symbols.

Equalization of CP-OFDM transmissions relies on the well-known property that every circulant matrix can be diagonalized by post- (pre-) multiplication by (I)FFT matrices (e.g., [24]). Indeed, after removing the CP at the receiver, and since the channel order satisfies  $L \leq D$ , (1) reduces to

$$\tilde{\mathbf{x}}_M(i) = \mathbf{C}_M(\mathbf{h}) \mathbf{F}_M^H \mathbf{s}_M(i) + \tilde{\mathbf{n}}_M(i) \quad (2)$$

where  $\mathbf{C}_M(\mathbf{h})$  is  $M \times M$  circulant matrix with first row  $\mathbf{C}_M(\mathbf{h}) := \text{Circ}_M(h_0 \ 0 \cdots 0 \ h_L \cdots h_1)$ , and  $\tilde{\mathbf{n}}_M(i) := [\tilde{n}(iP + D) \cdots \tilde{n}(iP + P - 1)]^T$ . Therefore, after demodulation with the FFT matrix, the “frequency domain” received signal is given by

$$\begin{aligned} \mathbf{x}_M(i) &= \mathbf{F}_M \mathbf{C}_M(\mathbf{h}) \mathbf{F}_M^H \mathbf{s}_M(i) + \mathbf{F}_M \tilde{\mathbf{n}}_M(i) \\ &= \text{diag}(H_0 \cdots H_{M-1}) \mathbf{s}_M(i) + \mathbf{F}_M \tilde{\mathbf{n}}_M(i) \\ &= \mathbf{D}_M \left( \tilde{\mathbf{h}}_M \right) \mathbf{s}_M(i) + \mathbf{n}_M(i) \end{aligned} \quad (3)$$

where  $\tilde{\mathbf{h}}_M = [H_0 \cdots H_{M-1}]^T = \sqrt{M} \mathbf{F}_M \mathbf{h}$ , with  $H_k \equiv H(2\pi k/M) := \sum_{l=0}^L h_l e^{-j2\pi kl/M}$  denoting the channel’s transfer function on the  $k$ th subcarrier;  $\mathbf{D}_M(\tilde{\mathbf{h}}_M)$  standing for the  $M \times M$  diagonal matrix with  $\tilde{\mathbf{h}}_M$  on its diagonal; and  $\mathbf{n}_M(i) := \mathbf{F}_M \tilde{\mathbf{n}}_M(i)$ .

This CP-OFDM property derives from the fast convolution algorithm based on the overlap–save (OLS) algorithm for block convolution [7]. It also enables one to deal easily with ISI channels by simply taking into account the scalar channel attenuations, e.g., when computing the metrics for the Viterbi decoder (as in Section III-C). However, it has the obvious drawback that the symbol  $s_k(i)$  transmitted on the  $k$ th subcarrier cannot be recovered when it is hit by a channel zero ( $H_k = 0$ ). This limitation leads to a loss in frequency (or multipath) diversity and can be overcome by the ZP precoder we review next [24].

### B. ZP-OFDM

The lower part of Fig. 1 depicts the baseband discrete-time block equivalent model of a ZP-OFDM system [11], [18], [24]. The only difference with CP-OFDM is that the CP is replaced by  $D$  trailing zeros that are padded at each precoded block  $\tilde{\mathbf{s}}(i)$  to yield the  $P \times 1$  transmitted vector  $\tilde{\mathbf{s}}_{zp}(i) = \mathbf{F}_{zp} \mathbf{s}_M(i)$ , where  $\mathbf{F}_{zp} := [\mathbf{F}_M \ \mathbf{0}]^H$ . The received block symbol is now given by

$$\tilde{\mathbf{x}}_{zp}(i) = \mathbf{H} \mathbf{F}_{zp} \mathbf{s}_M(i) + \mathbf{H}_{\text{IBI}} \mathbf{F}_{zp} \mathbf{s}_M(i-1) + \tilde{\mathbf{n}}_P(i) \quad (4)$$

and the key advantage of ZP-OFDM lies in the all-zero  $D \times M$  matrix  $\mathbf{0}$  which eliminates the IBI, since  $\mathbf{H}_{\text{IBI}} \mathbf{F}_{zp} = \mathbf{0}$ . Thus, letting  $\mathbf{H} := [\mathbf{H}_0, \mathbf{H}_{zp}]$  denote a partition of the  $P \times P$  convolution matrix  $\mathbf{H}$  between its first  $M$  and last  $D$  columns, the received  $P \times 1$  vector becomes

$$\tilde{\mathbf{x}}_{zp}(i) = \mathbf{H} \mathbf{F}_{zp} \mathbf{s}_M(i) + \tilde{\mathbf{n}}_P(i) = \mathbf{H}_0 \mathbf{F}_M^H \mathbf{s}_M(i) + \tilde{\mathbf{n}}_P(i). \quad (5)$$

Corresponding to the first  $M$  columns of  $\mathbf{H}$ , the  $P \times M$  submatrix  $\mathbf{H}_0$  is Toeplitz and is *always guaranteed to be invertible*, which assures symbol recovery (perfect detectability in the absence of noise) regardless of the channel zero locations [11], [18], [24]. This is not the case with CP-OFDM, and this is precisely the distinct advantage of ZP-OFDM. In fact, the channel-irrespective symbol detectability property of ZP-OFDM is equivalent to claiming that ZP-OFDM enjoys

maximum diversity gain [25]. In other words, ZP-OFDM is capable of recovering the diversity loss incurred by CP-OFDM [25]. Intuitively, this can be appreciated if one takes into account that ZP-OFDM removes IBI and retains the entire linear convolution of each transmitted block with the channel.

Assuming without loss of generality the symbols to have variance  $\sigma_s^2 = 1$ , the minimum norm ZF and MMSE equalizers for an additive white noise of variance  $\sigma_n^2$  are given, respectively, by [18]  $[(\cdot)^\dagger]$  denotes matrix pseudoinverse]

$$\mathbf{G}_{zf} = \mathbf{F}_M \mathbf{H}_0^\dagger, \quad \mathbf{G}_{\text{mmse}} = \mathbf{F}_M \mathbf{H}_0^H (\sigma_n^2 \mathbf{I}_P + \mathbf{H}_0 \mathbf{H}_0^H)^{-1}.$$

Note that both  $\mathbf{G}_{zf}$  and  $\mathbf{G}_{\text{mmse}}$  require, respectively, the inversion of either an  $M \times M$  or a  $P \times P$  matrix which cannot be precomputed since the matrix to be inverted depends on the channel. Hence, both the minimum norm ZF and the MMSE equalizers incur an extra implementation cost relative to the FFT-based CP-OFDM receiver. This observation motivates our subsequent low-complexity (albeit suboptimal) equalization schemes that target practical ZP-OFDM receivers.

### III. REDUCED COMPLEXITY EQUALIZATION SCHEMES FOR THE ZP PRECODER

In this section, two new equalization schemes will be developed, based on the circularity of the channel matrix. Both target reduced complexity by avoiding the inversion of a channel-dependent matrix. The first one relies on a  $P \times P$  circulant matrix which preserves the property of guaranteed symbol recovery and results only in a moderate performance degradation (Section III-A). The second one is based on an OLA approach, and relies on an  $M \times M$  circulant channel matrix (Section III-B). This reduces complexity further, but channel invertibility is not guaranteed anymore. Both novel equalizers will lend themselves naturally to the Viterbi decoding algorithm (Section III-C).

#### A. Fast Suboptimal Symbol Recovery: The ZP-FAST-MMSE Transceiver

The simplicity of CP-OFDM comes from the circularity of the channel matrix  $\mathbf{C}_M(\mathbf{h})$  in (2), which takes advantage of the FFT to yield a set of flat-fading subchannels that can be equalized easily. This feature is also present in the ZP precoder because, thanks to the trailing zeros, the last  $D$  columns of  $\mathbf{H}$  in (5) do not affect the received block. Thus, the Toeplitz matrix  $\mathbf{H}$  can be seen as a  $P \times P$  circulant matrix  $\mathbf{C}_P(\mathbf{h}) = \text{Circ}_P(h_0 \ 0 \cdots 0 \ h_L \cdots h_1)$ , and (5) can be rewritten as

$$\begin{aligned} \tilde{\mathbf{x}}_{zp}(i) &= \mathbf{H} \mathbf{F}_{zp} \mathbf{s}_M(i) + \tilde{\mathbf{n}}_P(i) \\ &= \mathbf{C}_P(\mathbf{h}) \mathbf{F}_{zp} \mathbf{s}_M(i) + \tilde{\mathbf{n}}_P(i). \end{aligned} \quad (6)$$

That way, the channel matrix can be diagonalized using the  $P \times P$  FFT matrix  $\mathbf{F}_P$  with entries  $\exp\{-j2\pi mk/P\}/\sqrt{P}$  as follows:

$$\begin{aligned} \mathbf{F}_P \mathbf{H} \mathbf{F}_{zp} &= \mathbf{F}_P \mathbf{C}_P(\mathbf{h}) \mathbf{F}_{zp} \\ &= \mathbf{F}_P \mathbf{C}_P(\mathbf{h}) \mathbf{F}_P^H \mathbf{F}_P \mathbf{F}_{zp} \\ &= \mathbf{D}_P \left( \tilde{\mathbf{h}}_P \right) \mathbf{F}_P \mathbf{F}_{zp} \\ &= \mathbf{D}_P \left( \tilde{\mathbf{h}}_P \right) \mathbf{V} \end{aligned} \quad (7)$$

TABLE I  
 ARITHMETIC COMPLEXITY COMPARISON IN THE HL2

	CP-OLS, TZ-OLA	TZ-FAST-ZF	TZ-FAST-MMSE	ZF, MMSE
Real multiplications	388	716	1196	15360
Real additions	1156	3532	4172	15518
Complex divisions	None	80	80	None

where  $\tilde{\mathbf{h}}_P := [H(0)H(2\pi/P) \cdots H(2\pi(P-1)/P)]^T = \sqrt{P}\mathbf{F}_P \mathbf{h}$ ,  $\mathbf{D}_P(\tilde{\mathbf{h}}_P)$  is the  $P \times P$  diagonal matrix with diagonal  $\tilde{\mathbf{h}}_P$ , and  $\mathbf{V}$  is a known  $P \times M$  structured matrix  $\mathbf{V} := \mathbf{F}_P \mathbf{F}_{zp}$ . Implementing the multiplication  $\mathbf{F}_P \tilde{\mathbf{x}}_{zp}(i) := \mathbf{x}_P(i)$  with a  $P$ -point FFT, the ZP-OFDM receiver output is

$$\begin{aligned} \mathbf{x}_P(i) &= \mathbf{F}_P \mathbf{H}_0 \mathbf{F}_M^H \mathbf{s}_M(i) + \mathbf{n}_P(i) \\ &= \mathbf{D}_P(\tilde{\mathbf{h}}_P) \mathbf{V} \mathbf{s}_M(i) + \mathbf{n}_P(i). \end{aligned} \quad (8)$$

Because the channel  $H(z)$  is of order  $L$ ,  $\mathbf{D}_P(\tilde{\mathbf{h}}_P)$  can have, at most,  $L$  zero-diagonal entries. However, unlike CP-OFDM, the remaining (at least  $P - L = M$ ) nonzero entries guarantee ZF recovery of  $\mathbf{s}_M(i)$  in ZP-OFDM, regardless of the underlying  $L$ th-order FIR channel nulls (note that any  $M$  rows of the matrix  $\mathbf{V}$  form a full-rank matrix). Inverting  $\mathbf{D}_P(\tilde{\mathbf{h}}_P) \mathbf{V}$  requires computing the pseudoinverse of a  $P \times M$  matrix, in general. Targeting low-complexity equalizers, we pursue two options.

*Option 1: (ZP-OFDM-FAST-ZF):* From (7), we can form a ZF equalizer in two steps after the  $P$ -point FFT  $\mathbf{F}_P$  is applied to  $\tilde{\mathbf{x}}_{zp}(i)$ . First, we obtain an estimate of  $\mathbf{y}_P(i) := \mathbf{V} \mathbf{s}_M(i)$  as  $\hat{\mathbf{y}}_P(i) = \mathbf{D}_P^\dagger(\tilde{\mathbf{h}}_P) \mathbf{x}_P(i)$ ; and then we find  $\hat{\mathbf{s}}_M(i) = \mathbf{V}^\dagger \mathbf{y}_P(i)$ , which leads to

$$\begin{aligned} \hat{\mathbf{s}}_M(i) &= \mathbf{V}^\dagger \mathbf{D}_P^\dagger(\tilde{\mathbf{h}}_P) \mathbf{x}_P(i) \\ &= \mathbf{s}_M(i) + \mathbf{V}^\dagger \mathbf{D}_P^\dagger(\tilde{\mathbf{h}}_P) \mathbf{n}_P(i). \end{aligned} \quad (9)$$

Because  $\mathbf{V}$  is not channel dependent, its pseudoinverse  $\mathbf{V}^\dagger$  can be precomputed, while in the operational mode, we only need to invert the diagonal  $\mathbf{D}_P(\tilde{\mathbf{h}}_P)$ . Moreover, we observe that  $\mathbf{V}^\dagger$  simply reduces to  $\mathbf{V}^\dagger = \mathbf{V}^H = \mathbf{F}_{zp}^H \mathbf{F}_P^H = [\mathbf{F}_M \mathbf{0}] \mathbf{F}_P^H$ . Thus, one can take advantage of the FFT to implement the multiplication of  $\hat{\mathbf{y}}_P(i)$  by  $\mathbf{V}^\dagger$ . Besides, with some existing OFDM systems (e.g., HL2),  $M$  is a power of two and  $L = M/4$ , and hence,  $P = 5(M/4)$  can be decomposed as the product of two coprime numbers: five and a power of two. Hence, the size  $P$  FFT can be implemented easily using five FFTs of size  $M/4$ , and  $M/4$  FFTs of size five without any additional operations such as multiplications by twiddle factors [8]. A table comparing the arithmetic complexity of the equalizers considered in this paper is provided in Table I in the case of HL2 (that is, for  $M = 64$  and  $P = 80 = 5 \times 16$ ). Since there is a plethora of implementations for complex divisions, we have deliberately chosen to not decompose them in terms of real additions and multiplications. Also, the arithmetic complexities for the ZF and MMSE equalizers only reflects the multiplication by  $\mathbf{G}_{zf}$  and  $\mathbf{G}_{mmse}$ . In other words, it does not reflect the evaluation of the underlying matrix inverses (in spite of their large complexities), because this is required only when the channel estimate is updated and not each time a block of symbols is received. We term the ZF equalization based on

(9) the ZP-OFDM-FAST-ZF algorithm. We underscore that this equalizer is not the minimum-norm ZF equalizer, because, in general,  $(\mathbf{D}_P(\tilde{\mathbf{h}}_P) \mathbf{V})^\dagger \neq \mathbf{V}^\dagger \mathbf{D}_P^\dagger(\tilde{\mathbf{h}}_P)$ . And symbol recovery will be impossible if the channel has a zero at one of the  $P$ -point FFT frequencies (or even when a zero is close to the  $P$ -point FFT grid) because the noise will be amplified in the first step.

*Option 2: (ZP-OFDM-FAST-MMSE):* To obtain a low-cost equalizer that mitigates the noise-enhancement problem, one could replace the first step in the ZP-OFDM-FAST-ZF by the MMSE estimator of  $\mathbf{y}_P(i) := \mathbf{V} \mathbf{s}_M(i)$  found using (8) as

$$\begin{aligned} \hat{\mathbf{y}}_P(i) &= \mathbb{E}[\mathbf{y}_P(i) \mathbf{x}_P^H(i)] \cdot \mathbb{E}^{-1}[\mathbf{x}_P(i) \mathbf{x}_P^H(i)] \\ &= \mathbf{V} \mathbf{V}^H \mathbf{D}_P(\tilde{\mathbf{h}}_P)^H \left[ \sigma_n^2 \mathbf{I} + \mathbf{D}_P(\tilde{\mathbf{h}}_P) \mathbf{V} \mathbf{V}^H \mathbf{D}_P(\tilde{\mathbf{h}}_P)^H \right]^{-1}. \end{aligned} \quad (10)$$

We can take the approximation  $\mathbf{V} \mathbf{V}^H \approx (N/P) \mathbf{I}$  and simplify (10) to  $\hat{\mathbf{y}}_P(i) = \mathbf{D}_P(\tilde{\mathbf{h}}_P) [(P/N) \sigma_n^2 \mathbf{I} + \mathbf{D}_P(\tilde{\mathbf{h}}_P) \mathbf{D}_P(\tilde{\mathbf{h}}_P)^H]^{-1}$ , which involves inversion of a diagonal matrix only. We term this equalizer ZP-OFDM-FAST-MMSE. At this point, we wish to reiterate that both options are computationally fast but, in general, they do not implement the minimum-norm solution of (8).

### B. Linking CP-OFDM With ZP-OFDM-OLA Transceivers

At the expense of channel-irrespective invertibility, one may pursue an alternative option at the receiver, which we term ZP-OFDM-OLA because it originates from the OLA method for block convolution (see also Fig. 1). Specifically, we can split  $\tilde{\mathbf{x}}_{zp}(i)$  in (5) into its upper  $M \times 1$  part  $\tilde{\mathbf{x}}_u(i) = \mathbf{H}_u \tilde{\mathbf{s}}_M(i)$  and its lower  $D \times 1$  part  $\tilde{\mathbf{x}}_l(i) = \mathbf{H}_l \tilde{\mathbf{s}}_M(i)$ , where  $\mathbf{H}_u$  ( $\mathbf{H}_l$ ) denotes the corresponding  $M \times M$  ( $D \times M$ ) partition of  $\mathbf{H}_0$ . Padding  $M - D$  zeros in  $\tilde{\mathbf{x}}_l(i)$  and adding the resulting vector to  $\tilde{\mathbf{x}}_u(i)$ , we can form

$$\begin{aligned} \tilde{\mathbf{x}}_M(i) &:= \tilde{\mathbf{x}}_u(i) + \begin{bmatrix} \tilde{\mathbf{x}}_l(i) \\ \mathbf{0}_{(M-L) \times 1} \end{bmatrix} \\ &= \left( \mathbf{H}_u + \begin{bmatrix} \mathbf{H}_l \\ \mathbf{0}_{(M-L) \times M} \end{bmatrix} \right) \tilde{\mathbf{s}}_M(i) := \mathbf{C}_M(\mathbf{h}) \tilde{\mathbf{s}}_M(i). \end{aligned} \quad (11)$$

Hence, (11) has exactly the same form as the CP-OFDM in (2), except that the OLA step colors slightly the noise term [not shown in (11)]. As in CP-OFDM, the circulant matrix  $\mathbf{C}_M(\mathbf{h})$  can be diagonalized by  $M \times M$  (D)FFT matrices, which leads to

$$\mathbf{F}_M \tilde{\mathbf{x}}_M(i) = \mathbf{F}_M \mathbf{C}_M(\mathbf{h}) \mathbf{F}_M^H \mathbf{s}_M(i) = \mathbf{D}_M(\tilde{\mathbf{h}}_M) \mathbf{s}_M(i). \quad (12)$$

ZF symbol recovery is then possible using  $\mathbf{s}_M(i) = \mathbf{D}_M^\dagger(\tilde{\mathbf{h}}_M) \mathbf{F}_M \tilde{\mathbf{x}}_M(i)$ .

From (12), we see that ZP-OFDM-OLA is equivalent to CP-OFDM, because they share the same overall  $M \times M$  transmitter transfer function  $\mathbf{D}_M(\tilde{\mathbf{h}}_M)$ . It is, thus, not surprising that it has identical complexity (two  $M$ -point FFTs are involved). This equivalence can easily be understood if both transceivers are redrawn as flow graphs [7]. ZP-OFDM-OLA is indeed the dual of CP-OFDM (which relies implicitly on the well-known OLS method as opposed to OLA) because its flow graph is simply the transpose of the CP-OFDM one.

### C. Equalization of Coded ZP-OFDM With Viterbi Decoding

In most existing OFDM systems, convolutional coding is implemented before the FFT precoder and the length- $I$  frame of equalized coded symbols  $\mathbf{s} = [\mathbf{s}_M^T(0), \dots, \mathbf{s}_M^T(I-1)]^T$  has to be decoded. To minimize BER, one has to search for the maximum-likelihood (ML) symbol estimates  $\hat{\mathbf{s}}_{\text{ML}} = \arg\max_{\mathbf{s}} P(\hat{\mathbf{s}}|\mathbf{s})$  subject to the code constraints (we consider here only the sequence of complex symbols  $\mathbf{s}$  instead of the sequence of information bits, thanks to the one-to-one mapping that exists between the two).

ML decoding is traditionally achieved in coded OFDM systems by first estimating the  $\hat{H}_k$  flat fades of each subcarrier, and then processing  $\mathbf{x}(i)$  instead of  $\hat{\mathbf{s}}(i) = \mathbf{D}_M^{-1}(\tilde{\mathbf{h}}_M)\mathbf{x}(i)$  to avoid the complex division [26]. Processing consists of factoring the probability  $P(\mathbf{x}|\mathbf{s})$  into marginal probabilities to reduce the ML search by taking advantage of the convolutional encoder linearity (e.g., by using Viterbi's algorithm [10]). Indeed, if the noise  $\tilde{n}_n(i)$  at the decoder input is AWGN with variance  $\sigma_n^2$ , the noise  $\mathbf{n}_M(i)$  after FFT is still AWGN with zero mean and covariance matrix  $\sigma_n^2 \mathbf{I}$  [cf. (3)]. Thus, one can decompose  $\log P(\mathbf{x}|\mathbf{s})$  into

$$\begin{aligned} \log P(\mathbf{x}|\mathbf{s}) &= \sum_{i=0}^{I-1} \log P(\mathbf{x}(i)|\mathbf{s}(i)) \\ &= \sum_{i=0}^{I-1} \sum_{k=0}^{M-1} \left| x_k(i) - \hat{H}_k^* s_k(i) \right|^2 - 2MI\sigma_n^2 \end{aligned} \quad (13)$$

which enables a very simple Viterbi decoding where all the transition metrics are simply added to obtain the path metrics (see, e.g., [10] for a detailed description).

We proved in (12) that similar to CP-OFDM, ZP-OFDM-OLA diagonalizes the channel. Hence, the decoding scheme in (13) can be readily applied to ZP-OFDM-OLA. Because the noise term is colored in ZP-OFDM-OLA, Viterbi decoding with metrics as in (13) only approximates the ML decoding. But FFT processing after OLA renders the colored noise approximately white, which enables application of the metric in (13). With respect to the other equalization schemes we mentioned in Section III-A, the issue of forming metrics for the Viterbi decoder is slightly more complicated, because one needs to account for the noise color at the demodulator output. Denoting by  $\mathbf{G}$  the matrix corresponding to the chosen ZP equalizer, the noise

covariance matrix is given by  $\mathbf{R}_{nn} = \sigma_n^2 \mathbf{G}\mathbf{G}^H$ , and  $P(\hat{\mathbf{s}}|\mathbf{s})$  can be expressed as

$$\begin{aligned} \log P(\hat{\mathbf{s}}|\mathbf{s}) &= \sum_{i=0}^{I-1} \log P(\hat{\mathbf{s}}(i)|\mathbf{s}(i)) \\ &= \sum_{i=0}^{I-1} [\hat{\mathbf{s}}(i) - \mathbf{s}(i)]^H (\mathbf{G}\mathbf{G}^H)^{-1} [\hat{\mathbf{s}}(i) - \mathbf{s}(i)] \\ &\quad - 2MI\sigma_n^2. \end{aligned} \quad (14)$$

Note that factoring out the probabilities to simplify the ML optimization in (14) is not as simple as in (13). A possible remedy could be to use a separate Viterbi for each subchannel, so that each one of them could be decoded independently. This has already been proposed in [9] for OFDM-CDMA systems and can be adopted here as well. However, this solution is best suited to multicarrier CDMA systems, because the information (hence, the coding) is spread over all subbands by a spreading matrix (e.g., a Walsh-Hadamard matrix), whereas it would result in a loss of diversity, and hence, reduction of the overall performance with the unspread CP or ZP-OFDM schemes considered herein.

This approximation is valid when a large-size interleaver is used, and is the one classically made in the literature when dealing with colored noise [note that ML decoding in presence of colored noise is a nontrivial problem (see, e.g., [1])]. This is equivalent to approximating the inverse of  $(\mathbf{G}\mathbf{G}^H)^{-1}$  by its main diagonal  $(\mathbf{G}\mathbf{G}^H)^{-1} \approx \text{diag}(g_1^{-1}, \dots, g_M^{-1})$ . The approximation accuracy increases with the size of the interleaver. That way, (14) becomes  $\log P(\hat{\mathbf{s}}|\mathbf{s}) \approx \sum_{i=0}^{I-1} \sum_{k=1}^M g_k^{-1} |\hat{s}_k(i) - s_k(i)|^2 - 2MI\sigma_n^2$ , and the same simplified Viterbi decoding as for CP-OFDM can be performed with only a small extra complexity added for computing the diagonal entries of  $(\mathbf{G}\mathbf{G}^H)^{-1}$ . The latter, though, is channel dependent, and has to be updated each time the channel varies.

## IV. NONLINEAR ISSUES

This section compares CP with ZP-OFDM in the presence of clipping effects. It is well known that the PA introduces nonlinear distortions, which destroy orthogonality between the carriers and deteriorate the overall system performance by introducing intercarrier interference [23]. The PA also introduces out-of-band interference which cannot be tolerated, because it affects adjacent systems. To reduce such interference, the complex symbols are often clipped in the digital domain before being transmitted. This clipping operation gives rise to in-band distortion [14]. For that reason, and even if correction methods have been developed [13], the symbols to be amplified are generally scaled by a factor  $\alpha < 1$  which limits the in-band distortion to an acceptable level. Because  $\alpha < 1$ , this reduces the operating signal-to-noise ratio (SNR), making the size of  $\alpha$  the pertinent figure of merit.

We will consider the simplified PA model in Fig. 1, where the PA is assumed to be linear up to a threshold and then saturates (thus inducing clipping effects), if the amplitude of the input signal is greater than the saturation level  $A$ . This model assumes that a digital predistorter has alleviated PA nonlinearities except for the in-band distortion introduced by the digital clipper. The *approximate clipping probability*  $\mathcal{C}$  is defined as

the number of clipped symbols over the total number of symbols per block.<sup>2</sup> One also defines the input backoff (IBO) as the ratio of the mean power at the PA input over the input saturation power  $A^2$  (which is assumed to be equal to  $\sigma_s^2$  in order to obtain a definition independent of the power level). The IBO is representative of the PA model and can be expressed in decibels as (cf. Fig. 1)  $\text{IBO}_{\text{dB}} = 10 \log \sigma_s^2 - 10 \log A^2 = 10 \log \alpha^2 \sigma_s^2 - 10 \log A^2 = 10 \log \alpha^2$ , where  $s^\alpha = \alpha \cdot s$ . In the next section, the approximate clipping probability will be considered as the figure of merit in order to determine which system requires the largest IBO (or, equivalently, the smallest  $\alpha$ ) to mitigate the in-band distortion.

In what follows, the  $i$ th frequency domain block  $\mathbf{s}_M(i)$  has entries drawn from a given constellation identically and independently distributed (i.i.d.) with variance  $\sigma_s^2 = 1$ . It is also well justified (especially for large  $M$ ) to approximate the probability density function (pdf) of the time domain symbol amplitude  $|\tilde{s}_k(i)|$  by a Rayleigh distribution, since the IFFT precoding present in both CP and ZP precoders maps the finite-alphabet sequence  $s_k(i)$ , to the approximately Gaussian i.i.d. sequence  $\tilde{s}_k(i)$  with Rayleigh distributed amplitudes  $p_s(r) = 2re^{-r^2}$ , except for the padded zeros in ZP-OFDM.

Because inserting the CP does not alter the pdf of the amplitudes, we infer that the symbols  $s_k^{\text{CP}}(i)$  have the same amplitude pdf as  $s_k(i)$ . Thus,  $\forall i$  the pdf of  $|\tilde{s}_k^\alpha(i)|$  after scaling is given by

$$p_{s^\alpha}(r) = \frac{1}{\alpha_{\text{CP}}} p_s\left(\frac{r}{\alpha_{\text{CP}}}\right). \quad (15)$$

In the ZP case, since the ZP part of each ZP-OFDM block is deterministically zero, and the pdf of  $|\tilde{s}_k^{\text{ZP}}(i)|$  is given by

$$p_{s^{\text{ZP}}}(r) = \frac{M}{P} p_s(r) = \frac{M}{P} 2re^{-r^2} + \frac{D}{P} \delta(r)$$

where  $\delta(r)$  is the Dirac delta function. The pdf of the scaled symbol amplitudes is

$$\begin{aligned} p_{s^\alpha}(r) &= \frac{M}{P} \frac{1}{\alpha_{\text{ZP}}} p_s\left(\frac{r}{\alpha_{\text{ZP}}}\right) \\ &= \frac{M}{P} \frac{2r}{\alpha_{\text{ZP}}} \exp\left(-\frac{r^2}{\alpha_{\text{ZP}}^2}\right) + \frac{D}{P} \delta(r). \end{aligned} \quad (16)$$

Recalling the definition of approximate clipping probability, we infer that for large enough block sizes it can be expressed as  $\mathcal{C} := \text{Prob}[\alpha r > A]$ . Because  $A = \sigma_s^2 = 1$  and  $\alpha^2 = 10^{-\text{IBO}/10}$ , we find using (15) and (16) that the approximate clipping probability for CP- and ZP-OFDM precoders can be expressed in terms of the IBO as follows:

$$\begin{aligned} \mathcal{C}_{\text{CP}} &= \int_1^{+\infty} \frac{2r}{\alpha_{\text{CP}}} \exp\left(-\frac{r^2}{\alpha_{\text{CP}}^2}\right) dr \\ &= \alpha_{\text{CP}} e^{-(1/\alpha_{\text{CP}}^2)} = 10^{(-\text{IBO}_{\text{CP}})/20} e^{-10^{\text{IBO}_{\text{CP}}/10}} \end{aligned}$$

and

$$\begin{aligned} \mathcal{C}_{\text{ZP}} &= \int_1^{+\infty} \frac{M}{P} \frac{2r}{\alpha_{\text{ZP}}} \exp\left(-\frac{r^2}{\alpha_{\text{ZP}}^2}\right) dr \\ &= \frac{M}{P} \alpha_{\text{ZP}} e^{-(1/\alpha_{\text{ZP}}^2)} = \frac{M}{P} 10^{(-\text{IBO}_{\text{ZP}})/20} e^{-10^{\text{IBO}_{\text{ZP}}/10}}. \end{aligned}$$

<sup>2</sup>Note that the clipping ratio which is traditionally considered in papers focusing on NL issues (see, e.g., [14]) is not relevant for a comparison between ZP and CP, since the transmitted symbols are not Gaussian in the ZP case.

With CP precoding and for small approximate clipping probabilities, the mean power of a block of symbols  $\tilde{\mathbf{s}}_{\text{CP}}(i)$  is approximately  $P\alpha_{\text{CP}}^2\sigma_s^2$ . Furthermore, the mean noise power corresponding to a block of symbols is  $P\sigma_n^2$ , and the equivalent SNR at the transmitter output for a given IBO is

$$\text{SNR}_{\text{CP}} = 10^{(-\text{IBO}_{\text{CP}})/10} \frac{\sigma_s^2}{\sigma_n^2}. \quad (17)$$

In the ZP case, the mean power transmitted during a block of symbols  $\tilde{\mathbf{s}}_{\text{ZP}}(i)$  is approximately  $M\alpha_{\text{ZP}}^2\sigma_s^2$  for small approximate clipping probabilities, while the mean noise power is  $P\sigma_n^2$ . Thus, the SNR at the transmitter output for a given IBO is given by

$$\text{SNR}_{\text{ZP}} = 10^{(-\text{IBO}_{\text{ZP}})/10} \frac{M}{P} \frac{\sigma_s^2}{\sigma_n^2}. \quad (18)$$

If we equate the IBOs by setting  $\alpha_{\text{ZP}} = \alpha_{\text{CP}}$ , then  $\mathcal{C}_{\text{ZP}} < \mathcal{C}_{\text{CP}}$  (since the zeros padded in ZP-OFDM are not clipped), while  $\text{SNR}_{\text{ZP}} < \text{SNR}_{\text{CP}}$  (because less power is transmitted in ZP-OFDM).

#### A. Impact on the Design of ZP-OFDM Systems

Standards always specify the out-of-band radiation to a given value which amounts to fixing the approximate clipping probability of the two precoders to a common value  $\mathcal{C} = \mathcal{C}_{\text{ZP}} = \mathcal{C}_{\text{CP}}$ . The two precoders then require different IBOs and their transmitter SNRs from (17) and (18) and can be related as

$$\text{SNR}_{\text{CP}} = \frac{P}{M} \text{SNR}_{\text{ZP}} 10^{-(\text{IBO}_{\text{CP}} - \text{IBO}_{\text{ZP}}/10)}. \quad (19)$$

The SNR difference  $\Delta_{\text{SNR}} := \text{SNR}_{\text{CP}} - \text{SNR}_{\text{ZP}}$  can be found from (19) as

$$\begin{aligned} \Delta_{\text{SNR}} &= 10 \log \left(1 + \frac{D}{M}\right) + \text{IBO}_{\text{ZP}} - \text{IBO}_{\text{CP}} \\ &\approx 10 \log \left(1 + \frac{D}{M}\right) \end{aligned}$$

where the last approximation holds for sufficiently small approximate clipping probabilities. The last equation reveals that for large enough block sizes  $M$  (relative to the CP length  $D$ ) ZP-OFDM has comparable behavior with CP-OFDM when it comes to clipping effects.

For the HL2 transmissions detailed in the next section,  $D/M = 0.25$ , and Fig. 2 shows that clipping effects alone require reducing the transmit power of ZP-OFDM by about 1 dB compared to CP-OFDM in order to guarantee the same out-of-band radiation, provided that the same power amplifier is used for both systems (the curve in Fig. 2 has been obtained by simulation, since one cannot express the SNR as a function of the approximate clipping probability in closed form). In other words, transmitting the same power level with both systems requires a PA with a clipping threshold slightly increased for ZP compared to CP, which is a minor price to pay for the benefit of guaranteed symbol recovery.

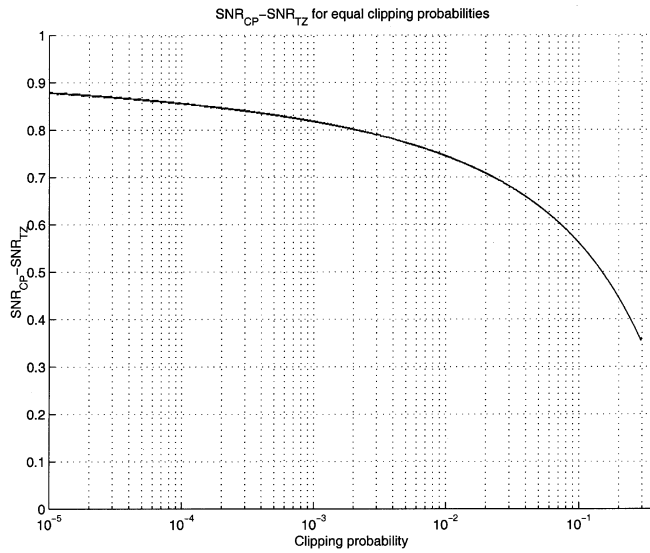


Fig. 2. SNR difference between CP and ZP induced by clipping effects.

## V. CHANNEL ESTIMATION ISSUES

This section deals with acquisition of CSI under the CP and ZP transmissions. It will turn out that the ZP precoder offers improved performance not only in CSI acquisition (Section V-A), but also in (semi) blind tracking of channel variations (Section V-B).

### A. CSI Acquisition

Channel estimation in CP-OFDM is usually performed in the frequency domain using pilot symbols [17], [21]. The channel transfer function  $H_k$  at each subcarrier  $\exp(j2\pi k/M)$  can be estimated from the noisy CP-OFDM symbols  $\mathbf{x}_M(i) = \mathbf{D}_M(\tilde{\mathbf{h}}_M)\mathbf{s}_M(i) + \mathbf{n}_M(i)$ . Specifically, by simply dividing the  $m$ th received symbol  $[\mathbf{x}_M(i)]_m$  by the  $m$ th pilot symbol  $[\mathbf{s}_M(i)]_m$ , we obtain from the  $i$ th received block

$$\begin{aligned} \hat{H}^{(i)}(2\pi m/M) &= \frac{[\mathbf{x}_M(i)]_m}{[\mathbf{s}_M(i)]_m} \\ &= H^{(i)}(2\pi m/M) + \frac{[\mathbf{n}_M(i)]_m}{[\mathbf{s}_M(i)]_m}, \\ & \quad m \in [0, M-1]. \end{aligned} \quad (20)$$

Since ZP-OFDM-OLA is equivalent to CP-OFDM, (20) applies directly to ZP-OFDM when one acquires CSI from the OLA receiver [cf. (11)]. Our simulations have confirmed that for a given receive SNR, the channel estimation accuracy with CP-OFDM is similar to that of ZP-OFDM-OLA, and their BER performance is, thus, comparable. However, when the channel's delay spread is longer than the CP, ZP-OFDM-FAST-MMSE exhibits improved BER performance over ZP-OFDM-OLA.

Because the ZP-OFDM-FAST options operate with the  $P$ -point FFT of the channel frequency response, they entail an extra  $M$ -point IFFT and a  $P$ -point FFT to retrieve  $H(2\pi p/P)$  from  $H(2\pi m/M)$ . However, a more direct channel estimator for ZP-OFDM is possible. Indeed, with  $\mathbf{v}_P(i) := \mathbf{V}\mathbf{s}_M(i)$ , a

channel estimate based on the  $i$ th received block can be found as [cf. (8)]

$$\hat{H}^{(i)}(2\pi p/P) = [\mathbf{x}_P(i)]_p / [\mathbf{v}_P(i)]_p, \quad p \in [0, P-1]. \quad (21)$$

For noise robustness, the pilot symbols in  $\mathbf{v}_P(i)$ , and hence, in  $\mathbf{s}_M(i)$ , need to be designed carefully [20]. A possible choice minimizing the MSE of  $\hat{H}^{(i)}(2\pi p/P)$  in (21) is to send the same pilot symbol on all subcarriers. The resulting MMSE for a channel with  $\|\mathbf{h}\|^2 = 1$  is then given by  $\epsilon_P^2 = E[(\mathbf{h} - \hat{\mathbf{h}})^H(\mathbf{h} - \hat{\mathbf{h}})] = \sigma_n^2 P/M$ , and is equal to the MMSE  $\epsilon_M^2$  of the channel estimated using the OLA structure. Furthermore, it is possible for both (20) and (21) to improve the  $\hat{H}^{(i)}(2\pi m/M)$  and  $\hat{H}^{(i)}(2\pi p/P)$  estimates by taking advantage of the fact that the channel is FIR of order  $\approx L \leq D$  [22]. This can be achieved by applying an IFFT to  $\hat{H}^{(i)}(2\pi m/M)$  or  $\hat{H}^{(i)}(2\pi p/P)$  for removing the spurious taps located after the CP, before switching back to the frequency domain. The MMSE of the resulting  $M$ - and  $P$ -sampled channel estimates for the ZP-OFDM-OLA and -FAST turns out to be, respectively

$$\epsilon_M^2 = \sigma_n^2 D P / M^2 \quad \epsilon_P^2 = \sigma_n^2 D / M = \epsilon_M^2 M / P < \epsilon_M^2.$$

Thus, for  $D = M/4$ , the fast equalizers for ZP-OFDM gain  $10 \log_{10}(P/M) = 0.96$  dB for channel estimation compared to the classical pilot-based method in [17].

### B. Channel Estimation Refinements

1) *Pilot-Based CSI*: Once the initial CSI has been acquired, it can be updated by sending pilot symbols on specific subcarriers and dividing the received symbols by the corresponding pilots as in (20) or (21). Furthermore, it is possible to capitalize on the continuous nature of the channel (the channels at different times or frequencies are correlated) to significantly improve this simple algorithm. Several time and/or frequency interpolation algorithms have already been proposed in the literature to reduce the noise influence and/or to update channel estimates between the pilot tones (see, e.g., [17] and references therein).

These algorithms, though originally developed for CP-OFDM, can be readily extended to ZP-OFDM, thanks to the OLA receiver that renders the two equivalent. However, pilot symbols are not always specified in the standards, or, they could be too distant either in frequency or in time to enable accurate updating of rapidly varying channels. Because it is important to track channel variations, an alternative (semi) blind approach is described next.

2) *Blind CSI Approaches*: Based on either CP- or ZP-based precoding, it is possible to identify blindly the channel from the received samples. We briefly outline next the ZP case only (the interested reader can find detailed derivations in [18] for the ZP precoder and in [16] for the CP precoder).

In the ZP case, the received block symbol is given by  $\tilde{\mathbf{x}}_P(i) = \mathbf{H}_0 \mathbf{F}_M^H \mathbf{s}_M(i) + \tilde{\mathbf{n}}_P(i)$ . Letting  $\mathbf{R} := E[\tilde{\mathbf{x}}_P(i) \tilde{\mathbf{x}}_P^H(i)]$  be the corresponding autocorrelation matrix, it follows that  $\text{rank}(\mathbf{H}_0) = M$  unless  $\mathbf{h} \equiv \mathbf{0}$ ; therefore, the noise subspace of  $\mathbf{R}$  has rank  $D$ . Denoting by  $\mathbf{G} = [\mathbf{g}_1 \cdots \mathbf{g}_D]$  a basis of this noise subspace,

it has been shown that  $\mathbf{h}$  is uniquely identifiable (within a scale) by solving the linear system of equations  $\mathbf{G}^{\mathcal{H}}\mathbf{H}_0 = \mathbf{0}$  [16].

Capitalizing on the commutativity of convolution, this system can be rewritten as  $\mathbf{h}^{\mathcal{H}}\mathcal{G} = \mathbf{0}$  by noticing that  $\mathbf{g}_i^{\mathcal{H}}\mathbf{H}_0 = [g_i(0) \cdots g_i(P-1)]^* \mathbf{H}_0 = \mathbf{h}\mathcal{G}_i^*$ , where  $\mathcal{G}_i$  is the  $D \times M$  Hankel matrix with first column  $[g_i(0) \cdots g_i(D)]^T$  and last row  $[g_i(D) \cdots g_i(P-1)]$ . In practice,  $\mathbf{R}$  is estimated by sample averaging  $\hat{\mathbf{R}}^{(N)} = N^{-1} \sum_{i=0}^{N-1} \tilde{\mathbf{x}}_P(i) \tilde{\mathbf{x}}_P^{\mathcal{H}}(i)$ , and therefore,  $\mathbf{G}^{\mathcal{H}}\mathbf{H}_0 = \mathbf{0}^{\mathcal{H}}$  has to be solved in the least-squares sense leading to the following quadratic optimization criterion:

$$\begin{aligned} \hat{\mathbf{h}} &= \underset{\mathbf{h}}{\operatorname{argmin}} \left( \sum_{i=0}^{D-1} \|\hat{\mathcal{G}}_i^{\mathcal{H}} \mathbf{h}\|^2 \right) \\ &= \underset{\mathbf{h}}{\operatorname{argmin}} \mathbf{h}^{\mathcal{H}} \left( \sum_{i=0}^{D-1} \hat{\mathcal{G}}_i \hat{\mathcal{G}}_i^{\mathcal{H}} \right) \mathbf{h}. \end{aligned} \quad (22)$$

The presence of null side carriers is not only specific to HL2, but it is a common feature of all current standardized OFDM systems (e.g., DAB and DVB). Presence of  $M - K$  virtual subcarriers implies that the autocorrelation matrix of  $\mathbf{s}_M(i)$  has rank  $K$  instead of  $M$ . This generates problems with existing subspace algorithms that cannot be applied directly. The required adjustments are detailed below.

With  $M - K$  virtual subcarriers, (3) must be replaced by  $\tilde{\mathbf{x}}_P(i) = \mathbf{H}_0 \mathbf{F}_{\text{tr}} \mathbf{s}_{\text{tr}}(i) + \tilde{\mathbf{n}}_P(i)$ , where  $\mathbf{F}_{\text{tr}}$  is the truncated  $M \times K$  matrix obtained from  $\mathbf{F}_M^{\mathcal{H}}$  by removing the columns corresponding to the zero entries of  $\mathbf{s}_M(i)$ . Correspondingly,  $\mathbf{s}_{\text{tr}}(i)$  includes the nonzero symbols of  $\mathbf{s}_M(i)$ . Hence, the channel estimates can be obtained by considering  $\mathbf{G}^{\mathcal{H}}\mathbf{H}_0 \mathbf{F}_{\text{tr}} = \mathbf{0}$  instead of  $\mathbf{G}^{\mathcal{H}}\mathbf{H}_0 = \mathbf{0}$ . Note that this equation leads to  $\mathbf{h}^{\mathcal{H}}\mathcal{G}\mathbf{F}_{\text{tr}} = \mathbf{0}^{\mathcal{H}}$  by commuting the vector–matrix product as before.

For the CP precoder, a similar subspace method has been presented in [16], but for brevity, the detailed derivation is skipped. The difference is that the size  $(P + M) \times (P + M)$  autocorrelation matrix of two successive overlapping blocks  $\tilde{\mathbf{x}}_P(i)$  and  $\tilde{\mathbf{x}}_P(i-1)$  has to replace the  $P \times P$  matrix  $\mathbf{R}$ . This increases complexity, because the autocorrelation matrix used by the ZP subspace algorithm is half the size of the one processed by the CP one. It also reduces the accuracy of the CP-based channel estimator, because the sample autocorrelation matrix used by the ZP-based approach reaches full rank with fewer samples than the CP one.

3) *Semiblind CSI Alternatives*: The semiblind algorithm of [16] applies directly to the present context. This algorithm accelerates convergence of the blind algorithm by taking advantage of the training sequence sent at the beginning of each burst to initialize the autocorrelation matrix estimation. However, it does not remove the scalar indeterminacy which is inherent to all blind methods. Indeed, the channel is identified by minimizing (22) subject to a properly chosen constraint to avoid the trivial (zero) solution. This estimates the channel up to a scalar coefficient  $\lambda \hat{\mathbf{h}}_{\text{sub}} = \lambda \hat{\mathbf{h}}$ , where  $\lambda$  can be inferred from the pilot carriers as we describe next.

Denote by  $X_1^{\text{pil}}, \dots, X_B^{\text{pil}}$  the symbols received on the  $B$  pilot subcarriers. Channel estimates at the corresponding frequencies are provided by

$$\hat{\mathbf{h}}_{\text{pil}} = \left[ X_1^{\text{pil}}/S_1^{\text{pil}}, \dots, X_B^{\text{pil}}/S_B^{\text{pil}} \right]^T \quad (23)$$

where  $S_1^{\text{pil}} \cdots S_B^{\text{pil}}$  denote the pilot symbols. A second set of estimates for these coefficients can be inferred from the subspace identification (up to  $\lambda$ )

$$\hat{\mathbf{h}}_{\text{sub}} = \mathbf{F}_{\text{pil}} \hat{\mathbf{h}}_{\text{sub}} = \lambda \mathbf{F}_{\text{pil}} \hat{\mathbf{h}} = \lambda \hat{\mathbf{h}} \quad (24)$$

where  $\mathbf{F}_{\text{pil}}$  is the matrix obtained from the  $M \times M$  FFT matrix  $\mathbf{F}_M$  by retaining only the  $B$  rows corresponding to the pilot carriers. Thus, using (23) and (24), we can determine  $\lambda$  by solving the linear system  $\hat{\mathbf{h}}_{\text{sub}} = \lambda \hat{\mathbf{h}}_{\text{pil}}$  in the least-squares sense. However, if the channel estimate  $\hat{\mathbf{h}}_{\text{sub}} = \lambda \hat{\mathbf{h}}$  obtained using the subspace algorithm is far from the true  $\mathbf{h}$  (up to  $\lambda$ ), the final channel estimates will remain inaccurate because knowledge of the channel on the pilot carriers is not exploited by the subspace algorithm. The latter can be achieved by considering the modified linear system

$$\begin{cases} \mathcal{G}_i^{\mathcal{H}} \mathbf{h} = \mathbf{0}^{\mathcal{H}}, & 1 \leq i \leq D \\ \mathbf{F}_{\text{pil}} \mathbf{h} = \hat{\mathbf{h}}_{\text{pil}}. \end{cases}$$

Since (24) holds only approximately in practice, it has to be solved in the least-squares sense similar to (22), which leads to the minimization of the following criterion:

$$\hat{\mathbf{h}} = \underset{\mathbf{h}}{\operatorname{argmin}} \left( \sum_{i=1}^D \|\hat{\mathcal{G}}_i^{\mathcal{H}} \mathbf{h}\|^2 + \|\mathbf{F}_{\text{pil}} \mathbf{h} - \hat{\mathbf{h}}_{\text{pil}}\|^2 \right). \quad (25)$$

The solution is  $\hat{\mathbf{h}} = (\mathbf{Q}_{\text{pil}})^{-1} \mathbf{F}_{\text{pil}}^{\mathcal{H}} \hat{\mathbf{h}}_{\text{pil}}$ , where  $\mathbf{Q}_{\text{pil}} = \sum_{i=1}^D \hat{\mathcal{G}}_i \hat{\mathcal{G}}_i^{\mathcal{H}} + \mathbf{F}_{\text{pil}}^{\mathcal{H}} \mathbf{F}_{\text{pil}}$ , and is related to the semiblind approach in [12]. The difference in our case is that often the training symbols alone cannot provide reliable channel estimates.

As illustrated in the simulations, the resulting semiblind algorithm combining all the aforementioned enhancements outperforms the classical pilot-based channel estimation algorithm for time-varying channels.

## VI. APPLICATION TO HIPERLAN/2

This section compares the performance of ZP-OFDM with that of CP-OFDM in the practical context of the HL2 (Section VI-A). Performance tests of the equalizers described in this paper are presented in Section VI-B assuming a time-invariant channel. Subsequently, time-varying channels are considered and the tracking capabilities of both precoders are compared in Section VI-C.

### A. Simulation Context

HL2 is a multicarrier system operating over 20 MHz in the 5-GHz band at typical SNR values of 0–25 dB for terminal speeds  $v \leq 3$  m/s. The number of carriers is  $M = 64$  and the CP has length  $D = 16$  samples. Among these  $M$  carriers, 12 carriers are null carriers (including the middle null corresponding to the dc component along with zeros padded at both ends in order to provide frequency guard bands against cochannel interference from adjacent OFDM systems). Among the remaining  $K = 52$  “central” subcarriers,  $B = 4$  are fixed pilots carrying known quaternary phase-shift keying (QPSK) symbols  $S_1^{\text{pil}} - S_4^{\text{pil}}$  while the rest “useful”  $U = K - 4 = 48$  subcarriers convey the information-bearing sequence.

With  $S$  denoting each of the 48 information symbols drawn from 4-, 16-, or 64-quadrature amplitude modulation (QAM) constellations (depending on the target BER), the corresponding frequency-domain OFDM symbol structure is

$$\left| \underbrace{0 \cdots 0}_6 \underbrace{S \cdots S}_5 S_1^{\text{pil}} \underbrace{S \cdots S}_{13} S_2^{\text{pil}} \underbrace{S \cdots S}_6 0 \right. \\ \left. \underbrace{S \cdots S}_6 S_3^{\text{pil}} \underbrace{S \cdots S}_{13} S_4^{\text{pil}} \underbrace{S \cdots S}_5 \underbrace{0 \cdots 0}_5 \right|.$$

The first two blocks of the burst  $s_M(0)$  and  $s_M(1)$  contain training symbols which are known to the receiver and can be used for CSI acquisition as described in Section V-A. Because only the entries  $m = 12, 26, 40, 54$  contain known symbols  $S_1^{\text{pil}} - S_4^{\text{pil}}$  in subsequent blocks  $s_M(i)_{i \geq 2}$ , one can track adaptively the channel transfer function using a running average (over, say,  $I = 10$  blocks) based only on these four carriers, as follows:

$$\hat{H}_m(i+1) = \frac{1}{I} \sum_{l=0}^{I-1} X_m(i-l) / S_m^{\text{pil}}(i-l), \\ m \in \{12, 26, 40, 54\}. \quad (26)$$

The HL2 standard specifies these four pilot carriers for synchronization and phase-tracking purposes, but they may be too distant in frequency (spaced more than the channel coherence bandwidth) for estimating the channel by a simple interpolation or even for tracking the channel variations. Thus, only partial channel tracking can be expected using (26), which may not yield accurate channel estimates in rapidly varying environments. To enhance mobility in HL2, semiblind channel estimation is well motivated, especially with the relatively small number of carriers that enable even subspace approaches to be tried with affordable complexity.

In what follows, the results are based on Monte Carlo simulations with each trial corresponding to a different realization of the typical 5-GHz channel models A and E specified by HL2 [4]. CSI is not available at the receiver and is estimated at the beginning of each frame using either the improved channel estimation method of Section V-A for ZP-OFDM, or the one in [17] for CP-OFDM.

### B. Comparing Equalization Capabilities

Figs. 3 and 4 depict BER for uncoded transmissions through channels A (fair channel) and E (difficult channel) as a function of the symbol SNR  $E_s/N_0$  for QPSK modulation and time-invariant channels. We infer that the guaranteed symbol recovery of the ZP precoder leads to significant performance gains of about 5 dB at  $10^{-3}$  BER when using the ZP-OFDM-MMSE equalizer. With our reduced complexity ZP-OFDM-FAST-MMSE equalizer, the guaranteed symbol recovery still affords a significant gain ( $\approx 3$  dB at  $10^{-3}$  BER). It can also be seen that the improvement is more pronounced for the channel with longer delay spread (Channel E), since the probability for a channel zero to be located on a subcarrier increases with the channel order (note the error floor at high

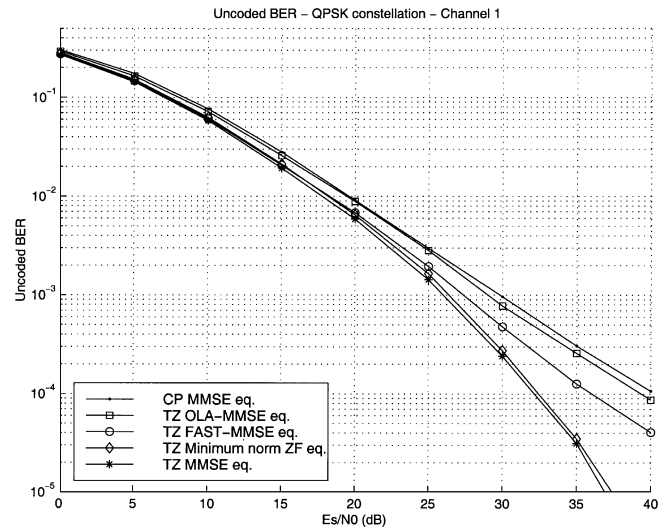


Fig. 3. Uncoded BER for the HL2 channel model A.

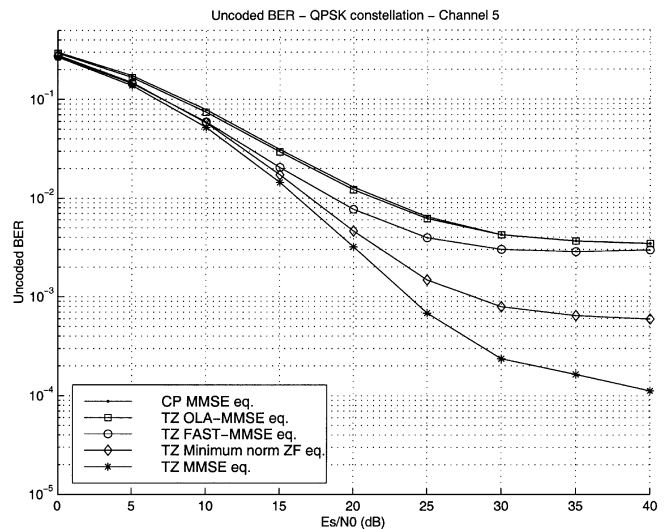


Fig. 4. Uncoded BER for the HL2 channel model E.

SNR is due to the fact that Channel E is longer than the amount of introduced redundancy).

Figs. 5 and 6 show the BER obtained when convolutional coding is implemented at the transmitter. The convolutional encoder is the one implemented in HL2 with rate  $R = 3/4$  and memory six defined in octal form by its two generator polynomials (133, 171). The curves illustrate that ZP-OFDM with its FAST or MMSE equalizers gains about 0.6 dB with Channel A and up to 1.5 dB with Channel E for a BER of  $10^{-2}$ , which is a significant gain for coded transmissions. They also show that the approximations made for enabling the trellis decoding (cf. Section III-C) do not affect significantly the performance gain brought by the various ZP equalizers.

Fig. 7 plots the estimated symbols MSE  $\epsilon^2 = (1/M) E_h[(s_M(i) - \hat{s}_M(i))^H (s_M(i) - \hat{s}_M(i))]$  as a function of SNR for the different ZP equalizers. The curve is obtained for different realizations of the Channel A (which is assumed here to be perfectly known) by computing for each equalizer the expression of the MSE  $\epsilon^2$  as a function of the CIR (the expectation being taken over the source symbols) and by

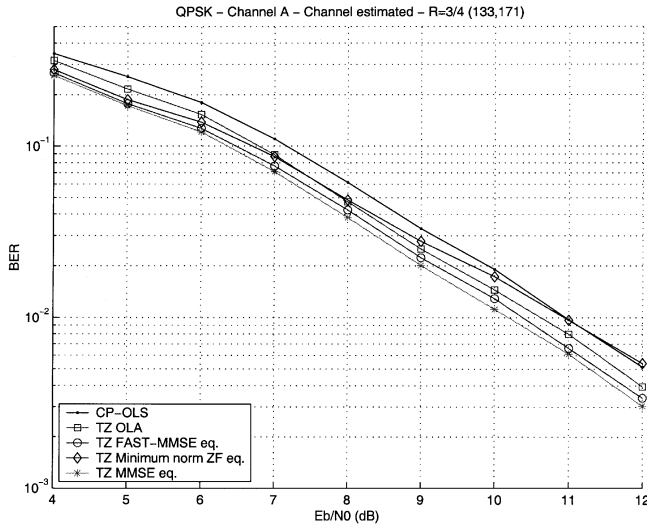


Fig. 5. Coded BER for the HL2 channel model A.

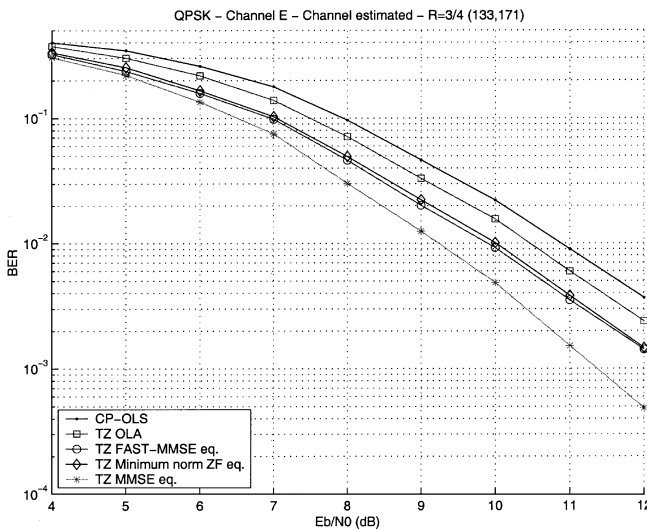


Fig. 6. Coded BER for the HL2 channel model E.

averaging the result over 1000 channel realizations. The curve corroborates that ZP-FAST-OFDM offers a good tradeoff between complexity and robustness to low SNR. Moreover, it also indicates that the numerical instability concerns with the ZP-MMSE equalizer mentioned in [18] (invertibility of matrix  $\sigma_n^2 \mathbf{I}_P + \mathbf{H}_0 \mathbf{H}_0^H$ ) are not present even at high realistic SNR values.

Thus, one may take advantage of the ZP-OFDM flexibility by designing a hybrid ZP-OFDM system which could first acquire the CSI and then choose the equalization scheme depending on the channel and on the operating SNR.

### C. Comparing Channel Estimation and Tracking Capabilities

To compare CP with ZP precoding in terms of channel estimation accuracy only, the performance criterion used in this section is channel mean-square error (MSE) defined as  $\text{MSE} = (1/U) \sum_{u \in \mathcal{U}} |H(2\pi u/M) - \hat{H}(2\pi u/M)|^2$ , where  $\mathcal{U}$  is the set of indexes corresponding to the  $U$  useful carriers (the MSE is only relevant on the  $U$  useful carriers, since only these subbands need to be equalized).

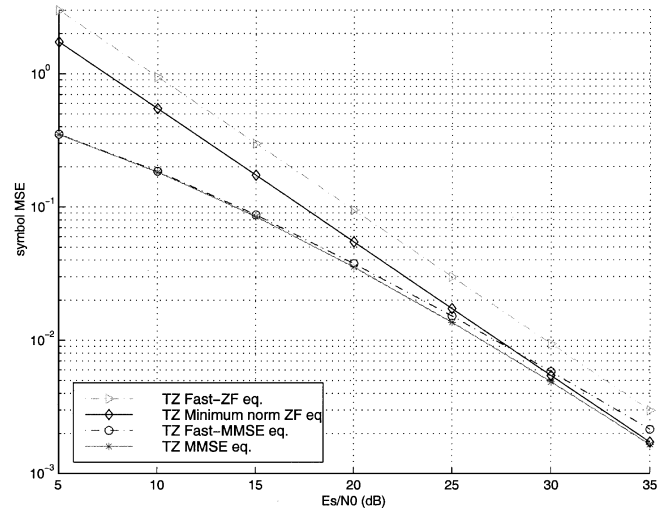


Fig. 7. Average symbol MSE for the ZP equalizers.

Moreover, in order to better quantify the impact of the channel estimation on the overall system performance, we use the following “effective SNR” criterion defined as [19]:

$$\text{SNR}_{\text{eff}} = -10 \log_{10}(10^{-\text{SNR}/10} + \text{MSE}). \quad (27)$$

This criterion can indeed be interpreted as the comprehensive SNR observed at the receiver by the Viterbi decoder, since the Viterbi algorithm decodes the transmitted symbol  $s_k(i)$  on subcarrier  $k$ , based on  $\hat{H}_k$ , by minimizing the metric  $m_k(i) = |x_k(i) - \hat{H}_k s_k(i)|^2 = |x_k(i) - H_k s_k(i) - \Delta(H_k) s_k(i)|^2$ , where  $\Delta(H_k)$  denotes channel estimation error. Because practical OFDM systems always implement frequency interleaving, the perturbation  $\Delta(H_k) s_k(i)$  can be approximated as AWGN. Therefore, it can be included in the thermal noise which justifies the criterion in (27). The effective SNR jointly takes into account the noise and the channel estimation error. However, it is important to recognize that this criterion only makes sense with CP-OFDM and ZP-OFDM-OLA and it is not appropriate to judge performance of coded transmissions with other transceivers based on the  $\text{SNR}_{\text{eff}}$  criterion of (27).

Fig. 8 illustrates the evolution of the channel’s MSE along the frame (which is 500 OFDM symbols long). It is clear that the channel estimates obtained from the pilot-based method degrade quickly when the channel is varying, whereas the subspace algorithms track its variations. Channel estimates are quickly more accurate for the ZP (by about 1 dB), which is reasonable, since the size of the autocorrelation matrix used by the ZP subspace algorithm is half the size of the one processed by the CP one.

Fig. 9 depicts the effective SNR in (27) averaged over the frame as a function of the thermal SNR. It shows that using the subspace algorithms enables a gain of about 0.5 dB at  $\text{SNR} = 5$  dB and 1.5 dB at  $\text{SNR} = 10$  dB compared to the standard method. Fig. 10 underlines the differences by illustrating the degradation of the effective SNR due to the channel estimation errors. It also highlights that the improved tracking capability of ZP further reduces the impact of the channel estimation error on the overall system performance.

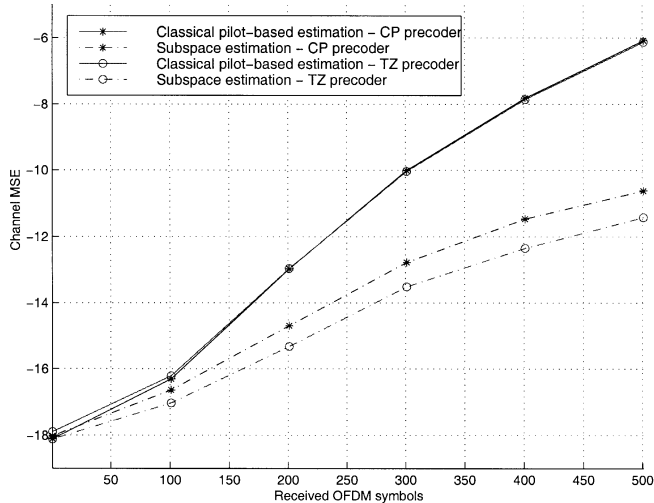
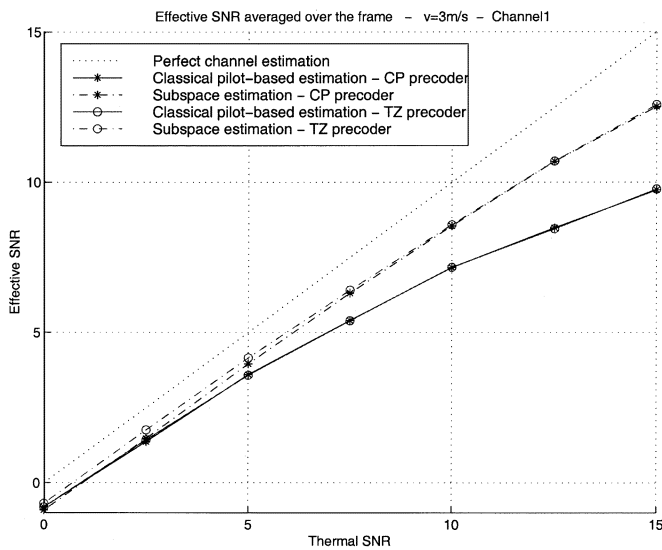
Fig. 8. Channel MSE at SNR = 10 dB,  $v = 3$  m/s.

Fig. 9. Average effective SNR versus the thermal noise.

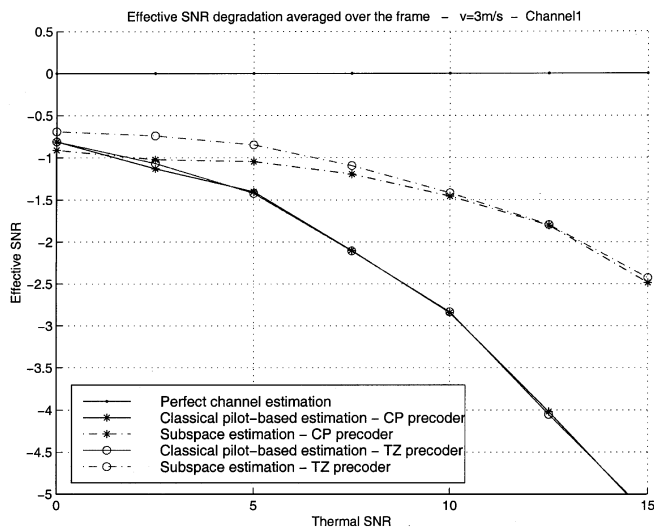


Fig. 10. Channel estimation errors.

The channels encountered in the HL2 standard vary only slowly and can be accurately estimated at the beginning of each frame using two pilot symbols. These reduce (but do not eliminate) the need for channel tracking. If the channel is varying faster, the benefit brought by the two subspace tracking algorithms would be more pronounced.

## VII. CONCLUSIONS

In a nutshell, we have demonstrated that the ZP-OFDM-FAST-MMSE equalizer of this paper outperforms the standard CP-OFDM with complexity lower than the ZP-OFDM-MMSE equalizer of [18]. With the fast equalizers developed herein, we have further evinced the merits of ZP-OFDM over CP-OFDM for wireless applications in the following facets:

- 1) channel-irrespective linear equalizability and guaranteed symbol recovery [11], [18];
- 2) flexibility in pursuing complexity-scalable ZP-OFDM variants such as OLA/FAST/MMSE combinations;
- 3) semiblind pilot-based channel estimation with improved tracking capability of channel variations.

In terms of PA-induced clipping effects, ZP introduces slightly more nonlinear distortions, and therefore, needs slightly increased power backoff than CP. At this point, among the subjects deserving further investigation is efficient time and frequency synchronization for ZP-OFDM so that it could be potentially considered for future multicarrier communication systems.

## REFERENCES

- [1] S. A. Alketa and J. K. Wolf, "Improvements in detectors based upon colored noise," *IEEE Trans. Magn.*, vol. 34, pp. 94–97, Jan. 1998.
- [2] ETSI Normalization Committee, "Radio Broadcasting Systems, Digital Audio Broadcasting (DAB) to mobile, portable and fixed receivers," Norme ETSI, Sophia-Antipolis, France, Doc. ETS 300 401, 1995–1997.
- [3] ETSI Normalization Committee, "Digital broadcasting systems for television, sound and data services; framing structure, channel coding and modulation for digital terrestrial television," Norme ETSI, Sophia-Antipolis, France, Doc. pr ETS 300 744, 1996.
- [4] ETSI Normalization Committee. (1998) Channel models for HIPERLAN/2 in different indoor scenarios. Norme ETSI, Sophia-Antipolis, France. [Online]. Available: <http://www.etsi.org>
- [5] ETSI Normalization Committee, "Broadband Radio Access Networks (BRAN); High Performance Radio Local Area Networks (HIPERLAN) type 2; System overview," Norme ETSI, Sophia-Antipolis, France, Doc. ETR0 230 002, Apr. 1999.
- [6] ANSI T1E1.4 Committee Contribution, "The DWMT: A multicarrier transceiver for ADSL using  $M$ -band wavelets," ANSI, Tech. Rep., Mar. 1993.
- [7] R. Crochiere and L. Rabine, *Multirate Digital Signal Processing*. Englewood Cliffs, NJ: Prentice-Hall, 1983.
- [8] P. Duhamel and M. Vetterli, "Fast Fourier transforms: a tutorial review and a state of the art," *Signal Processing*, no. 19, pp. 259–299, 1990.
- [9] K. Fazel and L. Papke, "On the performance of convolutionally-coded CDMA/OFDM for mobile communication system," in *Proc. IEEE PIMRC*, Yokohama, Japan, Sept. 1993, pp. 468–472.
- [10] G. Forney, "The Viterbi Algorithm," *IEEE Trans. Inform. Theory*, vol. IT-61, pp. 268–278, Mar. 1973.
- [11] G. B. Giannakis, "Filterbanks for blind channel identification and equalization," *IEEE Signal Processing Lett.*, vol. 4, pp. 184–187, June 1997.
- [12] A. Gorokhov and P. Loubaton, "Semiblind second-order identification of convolutive channels," in *Proc. IEEE Int. Conf. Acoustics, Speech, and Signal Processing*, vol. 5, Munich, Germany, Apr. 1997, pp. 3905–3908.

[13] A. L. Kambanellas and G. B. Giannakis, "Modulo pre-equalization of nonlinear communication channels," in *Proc. IEEE Workshop Signal Processing Advances for Wireless Communications*, Annapolis, MD, May 1999.

[14] X. Li and L. J. Cimini, "Effects of clipping and filtering on the performance of OFDM," *IEEE Commun. Lett.*, vol. 2, pp. 131–133, May 1998.

[15] J. Manton and Y. Hua, "A frequency domain deterministic approach to channel identification," *IEEE Signal Processing Lett.*, vol. 6, pp. 323–326, Dec. 1999.

[16] B. Muquet, M. de Courville, P. Duhamel, and V. Buzenac, "A subspace-based blind and semiblind channel identification method for OFDM systems," in *Proc. SPAWC'99*, May 1999, pp. 170–173.

[17] M. Sandell and O. Edfors, "A comparative study of pilot-based channel estimators for wireless OFDM," Lulea Univ. of Technol., Lulea, Sweden, Res. Rep. TULEA 1996, 1996.

[18] A. Scaglione, G. B. Giannakis, and S. Barbarossa, "Redundant filter-bank precoders and equalizers—Part I: Unification and optimal designs and Part II: Blind channel estimation, synchronization and direct equalization," *IEEE Trans. Signal Processing*, vol. 47, pp. 1988–2022, July 1999.

[19] M. Speth and H. Meyr, "Complexity constrained channel estimation for OFDM based transmission over fast fading channels," in *Proc. Eur. Personal Mobile Communications Conf.*, Paris, France, Mar. 1999, pp. 1639–1643.

[20] C. Tellambura, M. Parker, Y. J. Guom, S. Shepherd, and S. Barton, "Optimal sequences for channel estimation using discrete Fourier transform techniques," *IEEE Trans. Commun.*, vol. 47, pp. 230–238, Feb. 1999.

[21] V. Mignone and A. Morello, "CD3-OFDM: A novel demodulation scheme for fixed and mobile receivers," *IEEE Trans. Commun.*, vol. 44, pp. 1144–1151, Sept. 1996.

[22] J. van de Beek, O. Edfors, M. Sandell, S. Wilson, and P. Borjesson, "On channel estimation in OFDM systems," in *Proc. IEEE Vehicular Technology Conf.*, vol. 2, Chicago, IL, July 1995, pp. 815–819.

[23] R. van Nee and A. de Wilde, "Reducing the peak to average power ratio of OFDM," in *Proc. IEEE Vehicular Technology Conf.*, 1998, pp. 2072–2076.

[24] Z. Wang and G. B. Giannakis, "Wireless multicarrier communications: Where Fourier meets Shannon," *IEEE Signal Processing Mag.*, May 2000.

[25] Z. Wang and G. B. Giannakis, "Linearly precoded or coded OFDM against wireless channel fades?," presented at Proc. IEEE Workshop on Signal Processing Advances for Wireless Communications. [Online]. Available: <http://spincom.ece.umn.edu>

[26] W. Zou and W. Yiyan, "COFDM: An overview," *IEEE Trans. Broadcast.*, vol. 41, pp. 1–8, Mar. 1995.



**Zhengdao Wang** was born in Dalian, China, in 1973. He received the B.S. degree in electrical engineering and information science from the University of Science and Technology of China (USTC), Hefei, China, in 1996, and the M.Sc. degree in electrical engineering from the University of Virginia, Charlottesville, in 1998, and is currently working toward the Ph.D. degree in electrical and computer engineering at the University of Minnesota, Minneapolis.

His interests lie in the areas of statistical signal processing and communications, including cyclostationarity, blind equalization algorithms, transceiver optimization, multicarrier, wideband multiple rate systems, and coding. His current interests focus on design and optimization of wireless multiuser communication systems.



**Georgios B. Giannakis** (S'84–M'86–SM'91–F'97) received the Diploma in electrical engineering from the National Technical University of Athens, Athens, Greece, in 1981. He received the M.Sc. degree in electrical engineering, the M.Sc. degree in mathematics, and the Ph.D. degree in electrical engineering from the University of Southern California (USC), Los Angeles, in 1983, 1986, and 1986, respectively.

After lecturing for one year at USC, he joined the University of Virginia, Charlottesville, in 1987, where he became a Professor of Electrical Engineering in 1997. Since 1999, he has been a Professor with the Department of Electrical and Computer Engineering, University of Minnesota, Minneapolis, where he now holds an ADC Chair in Wireless Telecommunications. His general interests span the areas of communications and signal processing, estimation and detection theory, time-series analysis, and system identification, subjects on which he has published more than 140 journal papers, 270 conference papers, and two books. Current research topics focus on transmitter and receiver diversity techniques for single- and multiuser fading communication channels, precoding and space-time coding for block transmissions, multicarrier, and wideband wireless communication systems.

Dr. Giannakis is the corecipient of four best paper awards from the IEEE Signal Processing (SP) Society (1992, 1998, 2000, 2001). He also received the Society's Technical Achievement Award in 2000. He co-organized three IEEE-SP Workshops, and guest co-edited four special issues. He has served as Editor-in-Chief for the IEEE SIGNAL PROCESSING LETTERS, as Associate Editor for the IEEE TRANSACTIONS ON SIGNAL PROCESSING and the IEEE SIGNAL PROCESSING LETTERS, as secretary of the SP Conference Board, as a member of the SP Publications Board, as a member and Vice-Chair of the Statistical Signal and Array Processing Technical Committee, and as Chair of the SP for Communications Technical Committee. He is a member of the Editorial Board for the PROCEEDINGS OF THE IEEE, and the Steering Committee of the IEEE TRANSACTIONS ON WIRELESS COMMUNICATIONS. He is a member of the IEEE Fellows Election Committee, and the IEEE-SP Society's Board of Governors.



**Bertrand Muquet** (M'02) was born in France in 1973. He received the Ing. degree in electrical engineering from the Ecole Supérieure d'Electricité (Supélec), Gif sur Yvette, France, in 1996 and the teaching degree "Agrégration" in applied physics from the Ecole Normale Supérieure de Cachan, Cachan, France, in 1997. He received the Ph.D. degree from Ecole Nationale Supérieure des Télécommunications, Paris, France, in 2001.

He is currently with Stepmind, Boulogne, France, a company developing solutions in wireless transmissions (GSM, GPRS, EDGE, HIPERLAN/2, IEEE 802.11a). From 1998 to 2001, he was a Research Engineer working on OFDM systems at Motorola Laboratories, Paris, France. His general research interests lie in the area of signal processing and digital communications with emphasis on multicarrier and OFDM systems, blind channel estimation and equalization, and iterative and turbo algorithms.



**Marc De Courville** (M'98) was born in Paris, France, on April 21, 1969. He graduated from the Ecole Nationale Supérieure des Télécommunications, Paris, ("Engineering University") in 1993, and he received the Ph.D. degree in 1996 from the same institution.

Since 1996, he has been working for Motorola Laboratories, Paris, France, and is now a Research Team Manager involved in projects dealing with multicarrier systems for current and future generations of wireless local area networks. His research interests include digital communications and digital signal processing.



**Pierre Duhamel** (F'98) was born in France in 1953. He received the Ing. degree in electrical engineering from the National Institute for Applied Sciences (INSA) Rennes, France, in 1975, and the Dr. Ing. degree and the Doctoratès sciences degree in 1978 and 1986, respectively, both from Orsay University, Orsay, France.

From 1975 to 1980, he was with Thomson-CSF, Paris, France, where his research interests were in circuit theory and signal processing, including digital filtering and analog fault diagnosis. In 1980, he

joined the National Research Center in Telecommunications (CNET), Issy les Moulineaux, France, where his research activities were first concerned with the design of recursive CCD filters. Later, he worked on fast algorithms for computing Fourier transforms and convolutions, and applied similar techniques to adaptive filtering, spectral analysis and wavelet transforms. From 1993 to Sept. 2000, he was a Professor at the National School of Engineering in Telecommunications (ENST), Paris, France, with research activities focused on signal processing for communications. He was Head of the Signal and Image Processing Department from 1997 to 2000. He is now with CNRS/LSS (Laboratoire de Signaux et Systemes), Gif sur Yvette, France, where he is developing studies in signal processing for communications (including equalization, iterative decoding, multicarrier systems) and signal/image processing for multimedia applications, including source coding, joint source/channel coding, watermarking, and audio processing.

Dr. Duhamel was Chairman of the Digital Signal Processing Committee from 1996 to 1998, was an Associate Editor of the IEEE TRANSACTIONS ON SIGNAL PROCESSING from 1989 to 1991, and was Associate Editor for the IEEE SIGNAL PROCESSING LETTERS. He was a Guest Editor for the special issue of the IEEE TRANSACTIONS ON SIGNAL PROCESSING on wavelets. He was an IEEE Distinguished Lecturer for 1999, and was Co-General Chair of the 2001 International Workshop on Multimedia Signal Processing, Cannes, France. The paper on subspace-based methods for blind equalization, which he coauthored, received the Best Paper Award from the IEEE Signal Processing Society in 1998. He was awarded the "Grand Prix France Telecom" award by the French Science Academy in 2000.